GEOPHYSICAL RESEARCH LETTERS, VOL. 22, NO. 22, PAGES 3063-3066, NOVEMBER 15, 1995

Ocean-load tides at the South Pole: A validation of recent ocean-tide models

Duncan Carr Agnew
Institute of Geophysics and Planetary Physics, Scripps Institution of Oceanography
University of California, San Diego

Abstract. Small diurnal and semidiurnal gravity tides are seen at the South Pole because of the loading by and attraction of the ocean tides. These data provide a check on the quality of ocean-tide models, especially in the southernmost ocean, which has historically been the most lacking in tidal data. Ocean-tide models developed in the 1980's did not predict the gravity tides at this location very well. Recently-developed models based on the Topex/Poseidon altimetric data and improved hydrodynamical modeling agree much better with the observations, provided that the tides beneath the ice shelves are included. The level of agreement at this remote location suggests that, loads from very local tides aside, the new generation of ocean-tide models can predict the loading tides to very high accuracy.

Introduction

Measurements of the tides of the solid earth are significantly affected by the ocean tides, both through the loading from these tides and (for gravity and tilt) by the direct gravitational attraction of the shifting water mass. Precise measurements of the earth tides must thus be corrected for these effects (together termed "ocean loading") for such measurements to be useful in determining the earth's elastic structure; a knowledge of the loading effects is equally important in predicting the tidal motions, as must be done for the most precise geodetic measurements. A description of the ocean tides over the whole ocean (a "tidal model") has thus long been needed by the earth-tide and geodetic communities.

This need was first met in a reasonably satisfactory way in the early 1980's with the production of ocean tide models by Schwiderski (1978, 1983), which combined global coverage with enough detail (1° grid spacing) to be able to include some of the detail of tides near the coasts. Because these models were adjusted to fit coastal and island tide-gauge data, they were, in most coastal areas, fairly accurate, and thus satisfactory for computing ocean loads (which are usually dominated by the nearby tides). For these reasons, and also because these models were readily available in machine-readable form, they soon became the basis for most ocean-loading calculations.

Over the last few years, a number of new ocean-tide models have been developed, in large part to serve the needs of (and in turn use the data produced by) the satellite altimetric community. One line of development, which has been pursued by Le Provost and his coworkers at Grenoble, has been the production of a purely hydrodynamical model of tides for the world ocean, based on detailed finite-element modeling which includes many of the shelf seas (Le Provost *et al.*, 1994). Another has been the use of altimetric data to determine the tides. One of the first models developed from such data was that of Cartwright and Ray (1990), using Geosat data; the much-improved data from the Topex/Poseidon (T/P) mission has resulted in a large number of new models, some of which have been summarized by Le Provost *et al.* (1995).

Comparisons of these models with tidal constants from tide-gauges (especially using open-ocean, or "pelagic" constants) shows that the new models all fit the data considerably better than does the Schwiderski model; a series of intercomparisons between the various new models are in progress (Woodworth *et al.*, 1995; Shum *et al.*, 1995). My purpose here is to evaluate the new (and old) models against a set of observations that are especially sensitive to the tides in regions where gauge data are few and altimetric data absent: the southern oceans. The T/P data extend south only to latitude 66°S; while the Geosat data extended slightly further south, they are not of high quality because ice was often present. Tide-gauge data observations near and on the Antarctic coast are few, though they have been sufficient to show deficiences in the Schwiderski models in this region (Ray 1993). Another standard of comparison, which I have used here, is the observed gravity tides at the South Pole; while these are an integral over the models, this makes them a form of constraint somewhat complementary to the point measurements from tide gauges.

Observations

Observations of the gravity tide at the South Pole, using a LaCoste-Romberg earth-tide gravity meter, were begun under the sponsorship of L. Slichter in 1969 and have continued to the present. The motivation for these observations was primarily to study the earth's normal modes and long-period earth tides, but they also provide the most accurate estimates of ocean-load gravity tides available anywhere. At all other places where gravity tides have been measured, the signal at diurnal and semidiurnal periods is dominated by the body tides (the direct attraction of the Moon (or Sun), and the signal produced by the earth's elastic deformation). Since the accuracy of the estimate of the load tide is approximately the accuracy of the gravimeter calibration times the ratio of body to load tides (usually 50 or more), an extremely accurate calibration is needed to determine the load tide with any accuracy (Slichter, 1972; Baker *et al.*, 1991). But, if the body tide is zero, the load tide is known just as accurately as the gravimeter calibration; and, at the South Pole, the diurnal and semidiurnal body tides vanish. The load tides at the South Pole can thus be found with an accuracy of 1% or better, provided that there is adequate signal-to-noise.

Copyright 1995 by the American Geophysical Union.

Paper number 95GL03074
0094-8534/95/95GL-03074$03.00

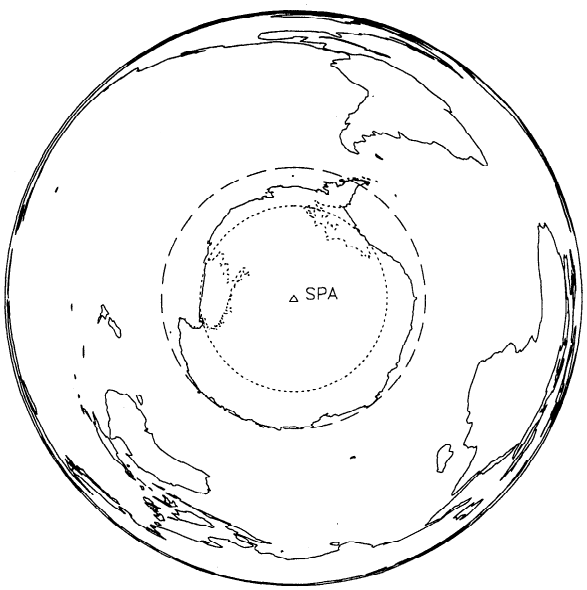

Figure 1. World map centered on station SPA (South Pole). The projection has been chosen so that a given thickness of water applied to an equal area on the map would give the same amount of gravitational attraction at SPA; the rule for this projection is that the radial distance plotted is proportional to $(\sin\Delta/2)^{1/2}$, where Δ is the distance in degrees (here, the North latitude plus 90°). The dashed circle shows the southern limit of T/P data, the dotted circle the southern limit of all models except for FES94.1 and FES95.2, and the dotted lines the boundaries of the ice shelves.

The diurnal and semidiurnal gravity tides at the South Pole have been discussed by Jackson and Slichter (1974), Rydelek and Zürn (1986) and Knopoff *et al.* (1989). The second of these showed that these tides were stable over time, and could be determined with a precision of about 0.07 nms^{-2} (0.007 μgal) for the diurnal tides and 0.03 nms^{-2} for the semidiurnal tides (relative precisions of 1% to 5%). The second of these papers compared these observations with the loads from the Schwiderski model, and found systematic differences, the diurnal tides being in general underpredicted and the semidiurnal ones overpredicted, suggesting serious inadequacies in these models in the southern ocean. Figure 1 is a world map projected in such a way that equal areas would have equal influence on gravity at the South Pole, given only the direct newtonian attraction of the extra mass (the elastic effects of such a load would exaggerate the size of the central region even more). The importance of the southern ocean is clear. The long-dashed line is the southern limit of T/P data, and shows one of the two regions (the other being the Arctic), over which ocean-tide models are currently little constrained by data.

Loading Computations

I have computed gravity load tides at the South Pole for a number of ocean-tide models, using a procedure very similar to that described in Knopoff *et al.* (1989). In all cases the Green function used was that found by Farrell (1972) for the Gutenberg-Bullen earth model; except at very close distances (not applicable here) this differs little from Green functions for newer earth models (Scherneck, 1990). An integrated Green-function method was used, the load being found for 1° bands, with the ocean tide taken to be constant within each cell of the model. Except in the case of the Schwiderksi models, mass conservation was not imposed; a direct check of this shows that the more recent models all satisfy this to within 1.5 mm, giving a maximum signal of 0.5 nms^{-2}.

Some of the salient points about the ocean models are listed in Table 1. A brief description of each would be:

1. Schwiderski: these models use a hydrodynamic interpolation between observed tidal values (mostly coastal). Some marginal seas are omitted.
2. SR94: these models were computed from 36 cycles of T/P data by direct Fourier analysis. The latitude limits, like those of other models using T/P data directly, are set by the latitude coverage of the T/P mission.
3. TPXO.2: these models were computed from the first 40 cycles of T/P data, by a data assimilation method which solves for dynamically admissible tides which satisfy these data. Because of the inversion technique used, the latitude coverage can extend south of the region of data availability.
4. FES94.1: these are the purely hydrodynamic models referred to above. Though they are computed using a finite-element model with variable mesh size, the distributed version has cells of fixed angular size. This is the first global ocean-tide model to include the regions under the Ross, Filchner, and Ronne ice shelves (outlined by dotted lines in Figure 1).
5. CSR3.0: these models were developed by taking the FES94.1 models, and correcting them using 89 cycles of T/P data. The correction was constrained to be smooth (with a smoothing width of about 7°), so that the original fine detail of the FES94.1 model was preserved, while regional corrections could be made. Outside the T/P latitude band, the models are relatively unchanged from the FES94.1 models.
6. FES95.2: these models were developed by adjusting the FES94.1 models using the CSR2.0 solution (Eanes, 1994) that was derived from the first year of T/P data, using an improved orbit.

As Table 1 shows, not all of the newer tide models are in fact global. Since the Arctic tides have little influence on the load tides at the South Pole, we may group the models by their southern limits. The SR94 models stop at the southern limit of T/P data; the Schwiderski, TPXO.2, and CSR3.0 models extend south to the limit of open water (though using very different

Table 1. Tidal Models

Name	Reference	Cell Dimensions (NS by EW)	Latitude Range	ftp Location
Schwiderski	Schwiderski (1978, 1983)	1° by 1 °	90°N—78°S	N/A
SR94	Schrama and Ray (1994)	1° by 1 °	66.5°N—67.5°S	ahab.gsfc.nasa.gov
TPXO.2	Egbert *et al.* (1994)	0.59° by 0.70°	70°N—78°S	ftp.oce.orst.edu
FES94.1	Le Provost *et al.* (1994)	0.5° by 0.5°	90°N—85°S	meolipc.img.fr
CSR3.0	(unpublished)	0.5° by 0.5°	90°N—78°S	ftp.csr.utexas.edu
FES95.2	(unpublished)	0.5° by 0.5°	90°N—85°S	meolipc.img.fr

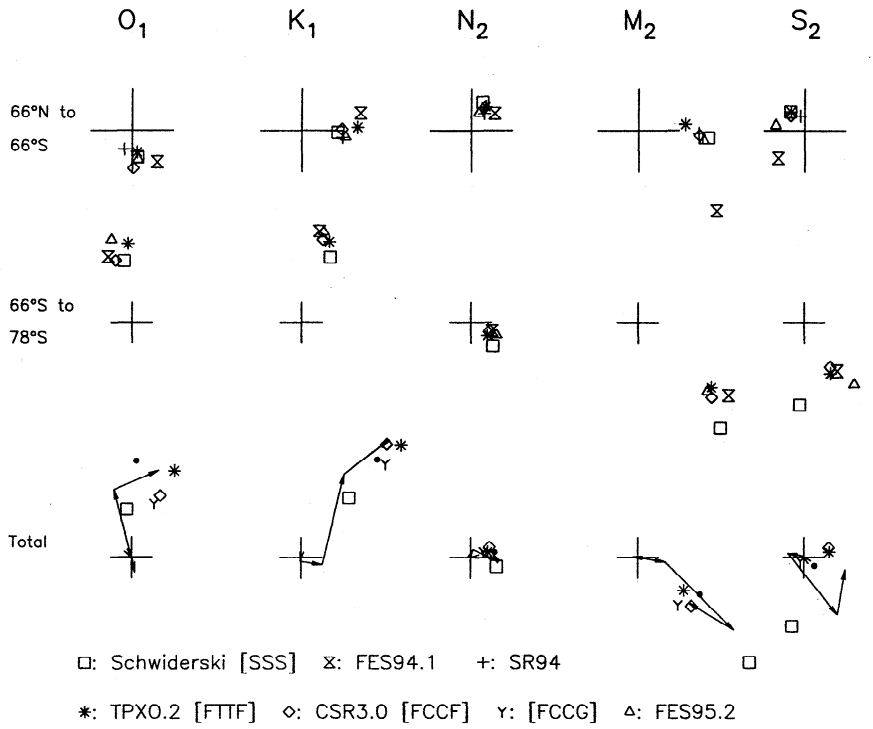

Figure 2. Phasor plots for the load tides at the South Pole. Phase is Greenwich, with lags negative; the arms of the cross are 1 nms^{-2} (0.1 μgal) long. The scale on the top row has been expanded. The solid dots on the bottom row are the observed results given by Rydelek and Zürn (1986); the errors are less than the size of the dots. The symbols are as defined, with the codes in brackets referring to the bottom row of plots (see Table 2). See text for further explanation.

methods to estimate the tides there); and the two FES models include the tides beneath the ice shelves. I have therefore computed the loads for the tides in four latitude bands: 90° N to 66°N (the Arctic), 66°N to 66°S (most of the world ocean), 66° to 78°S (open water south of the T/P limit), and south of 78°S (the ice shelves).

Results

With the number of models available for different latitude bands, there are a large number of combinations which can be used to estimate the total load. Figure 2 summarizes some of these, for the tidal constituents available for all models (most of the models include additional constituents). In all the subpanels, the tidal value (amplitude and phase) is shown as a phasor; the cross gives the scale. The top row shows the loads for the latitude band 66°N to 66°S. The loads from this region are about the same for all the T/P based models (and, perhaps surprisingly, for Schwiderski's). The only model that is substantially different is the purely hydrodynamic model FES94.1; a reflection, no doubt, of the known regional differences between this and other models (Le Provost *et al.*, 1995). It is clear that the adjustments applied to produce FES95.2 and CSR3.0 have corrected this discrepancy.

The second row gives the loads for the latitudes 66° to 78°S. All the newer models produce very similar loads; the Schwiderski models differ by a small amount, especially at M_2 and S_2. Of course, the area of ocean involved is not large (Figure 1), but the good agreement is certainly encouraging, given the lack of data for this region, and the fact that the TPXO.2 models estimate the tides there in a way completely independent from that used in FES95.2 and CSR3.0.

Finally, the third row shows the total load at the South Pole, both observed (the solid dot) and computed. The series of arrows show how the different latitude bands contribute for the FES95.2 models; for the other combinations only the symbol for the sum is shown. For all the newer models the misfit to the data (Table 2) is much less than for the Schwiderski models. Much, but not all, of this improvement can be credited to including the ice-shelf tides; as has recently been pointed out by Melchior (1995) these are important at this location, although his suggestion that the geologic structure of Antarctica might also account for this discrepancy seems unwarranted given the generally excellent fit.

However, it is also clear that the models for the rest of the ocean have converged to give answers that match the observations as well as can be expected (especially given the

Table 2. Misfits of Computed Load Tides

Models	Tidal Constituent				
	O_1	K_1	N_2	M_2	S_2
SSS	2.41	2.32	0.72	4.09	3.12
FFFF	1.17	1.12	0.13	0.67	1.53
FCCF	2.07	0.88	0.35	0.70	1.13
FCCG	2.27	0.44	0.54	1.19	0.73
FTTF	1.92	1.34	0.34	0.82	0.99

Amplitude of misfit vector, in nms^{-2}; to convert to elevation in mm multiply by 0.3. Model codes are: S—Schwiderksi, F—FES95.2, C—CSR3.0, T—TPXO.2, G—FES94.1. Order is four latitude bands described in text (e.g., in the next to last line FES94.1 has been used for the ice-shelf tides, and for all but the Schwiderski model, FES95.2 has been used for the Arctic tides.).

uncertainty in the ice-shelf tides). As Table 2 shows, no one model, or combination of models, can be said to be superior for all tidal constituents (other than in the simple sense that those models that do not extend far enough south need to be supplemented). The largest misfits overall seem to be at O_1 and S_2; the latter might well reflect atmospheric pressure tides affecting the gravity data.

Conclusions

The results given here suggest that the ocean tides for the region south of 66°S latitude are, if not perfectly known, fairly well determined in recent models. This includes the tides beneath the ice shelves; indeed, this is perhaps the most impressive achievement of the FES models, given the poorly-known bathymetry and the lack of data in the area. While the South Pole data are not a particularly good test of tidal models for regions further north, enough other tests are being conducted (Woodworth *et al.*, 1995) to show that these models do satisfy the available "ground-truth" quite well.

This in turn suggests a conclusion relevant to the study of earth tides. In so far as the ocean tides are well determined, the ocean-loading contribution to earth tides is also: just as has long been true for the body tides, we can then regard these as something we can compute *a priori*, rather than a means of finding out about the earth. The results here suggest that the pelagic tides are well determined even south of the area covered by altimetry; the above argument would thus apply over most of the world. While there are shallow areas where the complexity of the tides cannot be captured as easily by the coarse spatial resolution of satellite altimetry, these "littoral tides" can be studied much more directly by altimetry, bottom-pressure measurements, and hydrodynamic modeling, than from earth-tide data. It would appear that, just as seismology has largely outstripped earth tides as a means of determining earth structure, so satellite altimetry has for the ocean tides.

Acknowledgments. Obviously, without the devoted efforts of many people who ran the UCLA gravimeter at the South Pole, and also the management and funding efforts of Louis Slichter and Leon Knopoff, there would be nothing to write about. I thank Richard Ray for help in getting me (re)started in this field, for a number of helpful discussions, and especially for letting me know of the Internet locations of a number of tidal models. Naturally, I also thank all those investigators who have made their models freely available on the Internet, and clearly documented to boot; I especially thank Rodney James and Richard Eanes for help and advice. I also thank Walter Zürn and Trevor Baker for discussions. This research was supported by the NASA DOSE program.

References

Baker, T. F., R. J. Edge, and G. Jeffries, Tidal gravity and ocean tide loading in Europe, *Geophys. J. Int., 107*, 1-11, 1991.

Cartwright, D. E., and R. D. Ray, Oceanic tides from Geosat altimetry, *J. Geophys. Res., 95*, 3069-3090, 1990.

Eanes, R. J., Diurnal and semidiurnal tides from TOPEX/POSEIDON altimetry, *Eos Trans. AGU, 1994 Spring Meeting Suppl.*, 108, 1994.

Egbert, G. D., A. F. Bennett, and M. G. G. Foreman, TOPEX/POSEIDON tides estimated using a global inverse model, *J. Geophys. Res., 99*, 24821-24852, 1994.

Farrell, W. E., Deformation of the earth by surface loads, *Rev. Geophys. Space Phys., 10*, 761-797, 1972.

Jackson, B. V., and L. B. Slichter, The residual daily earth tides at the South Pole, *J. Geophys. Res., 69*, 1711-1715, 1974.

Knopoff, L., P. A. Rydelek, W. Zürn, and D. C. Agnew, Observations of load tides at the South Pole, *Phys. Earth Planet. Inter., 54*, 33-37, 1989.

Le Provost, C., M. L. Genco, F. Lyard, P. Vincent, and P. Canceil, Spectroscopy of the world ocean tides from a finite element hydrodynamic model, *J. Geophys. Res., 99*, 24777-24797, 1994.

Le Provost, C., A. F. Bennett, and D. E. Cartwright, Ocean tides for and from TOPEX/POSEIDON, *Science, 267*, 639-642, 1995.

Melchior, P., A continuing discussion about the correlation of tidal gravity anomalies and heat flow densities, *Phys. Earth Planet. Inter., 88*, 33-37, 1995.

Ray, R. D., Global ocean tide models on the eve of TOPEX/POSEIDON, *IEEE Trans. Geosc. Remote Sens., 31*, 355-364.

Rydelek, P., and W. Zürn, Analysis of anomalous tides at the South Pole, in *Proceedings 10th International Symposium on Earth Tides*, edited by R. Viera, pp. 817-826, Consejo Superior de Investigaciones Cientificas, Madrid, 1986.

Scherneck, H.-G., Loading Green's functions for a continental shield with a Q-structure for the mantle and density constraints for the geoid, *Bull. Infor. Mar. Terr, 108*, 7775-7792, 1990.

Schrama, E., and R. D. Ray, A preliminary tidal analysis of TOPEX/POSEIDON altimetry. *J. Geophys. Res., 99*, 24799-24808, 1994.

Schwiderski, E. W. Global Ocean Tides, Part I: a detailed hydrodynamical interpolation model. *NSWC Tech. Rept.*, Naval Surface Weapons Center, Dahlgren, VA, 1978.

Schwiderski, E. W. Atlas of ocean tidal maps and charts I: the semidiurnal principal lunar tide M_2, *Mar. Geodesy, 6*, 219-265, 1983.

Shum, C. K., C. Le Provost, and P. Woodworth, May 1995 recommendation of TOPEX/POSEIDON ocean tide model, WWW document, URL http://biudc.nbi.ac.uk/altim/topex.may.report.html, 1995.

Slichter, L. B. Earth tides, in *The Nature of the Solid Earth*, edited by E. C Robertson, pp. 285-320, McGraw-Hill, New York, 1974.

Woodworth, P., C. Le Provost, and C. K. Shum, Interim recommendation of TOPEX/POSEIDON tide model, 6 February 1995, WWW document, URL http://biudc.nbi.ac.uk/altim/tide.models.html, 1995.

D. C. Agnew, U. C. San Diego, IGPP-0225, 9500 Gilman Drive, La Jolla, CA 92093-0225. (e-mail: dagnew@ucsd.edu)

Received: August 16, 1995 Accepted: September 15, 1995